A FLAMELET MODEL FOR END OF DIFFUSION FLAMES IN POROUS MEDIUM

Max A.E. Kokubun, max@lcp.inpe.br
Fernando F. Fachini, fachini@lcp.inpe.br
Laboratório de Combustão e Propulsão - INPE, Cachoeira Paulista-SP

Abstract. *In the present work, a flamelet-type modeling is made for describing the features of liquid fuel combustion, at it's final stage, inside a porous inert medium. The flamelet theory has been formulated for describing a flame element for turbulent combustion, and is one of the tools for studying flame dynamics. Combustion established inside a porous medium has some features that are not observable at free propagating combustion. First of all, one must consider that the porous matrix acts as a resistance force to the flow due to the tortuosity, which is taken into account in the conservation equations. Also, the porous matrix interacts directly with the system recirculating the heat upward and downward the reaction zone, leading to a more efficient burning process, and, consequently, with less pollutant combustion emission. In the present work we consider the final stage of a diffusion flame established inside the porous medium, where the remaining fuel is a heavy, very low volatile one, in which the remaining physical process is a lower order vaporization, not enough to sustain the flame. We model our system using assumption of a very low volatility fuel, low permeability porous medium and use boundary-layer approximation. The vaporization rate is estimated, and temperature profiles for the three existing phases are obtained, so as the momentum profile for the flowing gas. Asymptotic theory was used as the mathematical approach.*

Keywords: *diffusion flames, porous medium, flamelet, heavy-fuel*

1. INTRODUCTION

Combustion phenomena inside porous medium have been studied for decades (Howell et al., 1996; Kayal and Chakravarty, 2005). Such interest may be explained by the enormous amount of applications encountered for these combustion systems, ranging from industrial chambers, passing by in-situ oil recovery to household applications (Mujeebu et al., 2008). One of the main features related to porous media confined combustion is the heat recirculation from downstream to upstream the flame, such characteristic provides an excess enthalpy to preheat the reactants, leading then to a more efficient combustion process, and even making it possible to burn lean mixtures. Also one may observe improvement in the excess temperature, making the process of porous media confined combustion more efficient than free one.

In the present work, a post-combustion, heavy-fuel evaporating regime established inside a porous medium is studied. Such situation appears, for example, after in-situ combustion have been performed in oil wells. The propagation of a combustion front in wells is used as a thermal recovery of heavy oil (Castanier and Brigham, 2003). After the front have passed, the remaining fuel left behind is the heaviest part of the oil, and it contains undesirable impurities. But since the well is still hot, this remaining heavy fuel may continue to vaporize, establishing a regime similar to the one presented in this work.

The physical configuration to be considered, when analyzed from the flamelet scope, is an impinging hot oxidant stream over a pool of liquid fuel, as seen below:

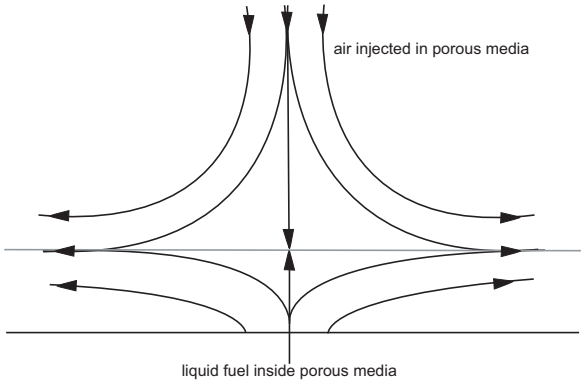

Figure 1. Evaporating fuel

We assume that the flame have extinguished and the remaining fuel is heavy and very low-volatile. At this configuration, we observe the low vaporization regime.

When the flow impinges at the liquid surface, a stagnation-point-kind of flow configuration is established. In a free impinging flow system, the evaporating regime is non-efficient. But when we add the porous matrix, the solid carries the heat to inside the liquid fuel, due to the high value of thermal conductivity, if compared to the gas.

The gas-solid problem have a field solution very similar to the field created by a stagnation-point flow (Wu et al., 2005). Analyzing the liquid-solid problem, we find two distinct zones: a equilibrium region, where the temperatures for solid and liquid are equal, and a boiling zone, where the liquid have a constant temperature near it's boiling temperature and the solid continue to raise its temperature, since it has no upper limit. In this boiling zone the profiles are decoupled, and such thermal difference is the main responsible for providing the necessary heat for the fuel phase change. In the present work we assume that all heat used to vaporize the fuel comes from the liquid-solid thermal interaction.

The proposed model uses asymptotic theory to obtain analytical expressions for the entire gas, liquid and solid coupled problems. The obtained results will be discussed in physical grounds.

2. MATHEMATICAL FORMULATION

In the proposed model, we utilize conservation equations for both regions, liquid-solid and gas-solid. Non-dimensional variables are given by: $u \equiv \bar{u}/\bar{v}_\infty$, $\varrho \equiv \rho/\rho_\infty = 1$, $\varrho_l \equiv \rho_l/\rho_\infty$, $v \equiv \bar{v}/\bar{v}_\infty$, $v_l \equiv \bar{v}_l/\bar{v}_\infty$, $p \equiv \bar{p}/(\rho_\infty v_\infty^2)$, $x \equiv \bar{x}/l_c$, $z \equiv \bar{z}/l_c$, $a \equiv (l_c/\bar{v}_\infty)d\bar{u}/d\bar{x}|_\infty$, $\theta_g \equiv T_g/T_\infty$, $\theta_s \equiv T_s/T_\infty$, $\theta_l \equiv T_l/T_\infty$, $y_O \equiv Y_O/Y_{O\infty}$ and $y_F \equiv Y_F$.

And the transformations used are:

$$u = a\, x\, U(z), \quad \varrho\, v = -a^{1/2} f,$$

$$p_0 - p = \frac{1}{2} Pr\, a^2 \left(1 + \frac{1}{\Gamma}\frac{l_c^2}{aK}\right)\left(x^2 + \frac{2F(z)}{a}\right), \quad \eta = \varrho a^{1/2} z$$

Above, p_0 is the stagnation pressure and l_c is a characteristic length scale, defined by $l_c = \bar{\lambda}_s/(\rho_\infty c_p \bar{v}_\infty)$.

In the following, the non-dimensional conservation equations are presented with the transformations already performed. First, the mass conservation equation:

$$U = \frac{df}{d\eta} \tag{1}$$

The momentum conservation equation is given by:

$$\frac{Pr}{\Gamma}\frac{d^3 f}{d\eta^3} + f\frac{d^2 f}{d\eta^2} - \left(\frac{df}{d\eta}\right)^2 - \varepsilon\frac{Pr}{\kappa\Gamma}\frac{df}{d\eta} = -\varepsilon Pr\left(1 + \frac{1}{\kappa\Gamma}\right) \tag{2}$$

Pr is the Prandtl number and $\Gamma \sim 60$ is a ratio between solid and gas thermal conductivities. κ is a non-dimensional permeability and it is assumed to be proportional to $1/\Gamma^2$.

The species conservation are presented as:

$$\frac{1}{\Gamma}\frac{d^2 y_F}{d\eta^2} + L_F f\frac{dy_F}{d\eta} = 0 \tag{3}$$

$$\frac{1}{\Gamma}\frac{d^2 y_O}{d\eta^2} + L_O f\frac{dy_O}{d\eta} = 0 \tag{4}$$

Where the Lewis numbers appears, connecting mass and thermal diffusion.

The energy equation are presented next, both for the gas and solid matrix filled with gas:

$$\varepsilon\frac{1}{\Gamma}\frac{d^2\theta_g}{d\eta^2} + \varepsilon f\frac{d\theta_g}{d\eta} = -\frac{N_v}{a}\,(\theta_s - \theta_g) \tag{5}$$

$$0 = (1-\varepsilon)\frac{d^2\theta_s}{d\eta^2} - N_v\frac{1}{a}(\theta_s - \theta_g) \tag{6}$$

The following boundary conditions must be obeyed:

$$\frac{df}{d\eta} - 1 = \theta_g - 1 = \theta_s - 1 = y_O - 1 = y_F = 0 \text{ for } \eta = \infty$$

At the liquid surface $\eta = 0$, the boundary conditions are

$$\frac{df}{d\eta} = f - f_0 = \theta_g - \theta_b = \theta_s - \theta_{s0} = y_O = y_F - y_{F0} = 0, \quad \frac{1}{\Gamma}\frac{1}{L_F}\left.\frac{dy_F}{d\eta}\right|_{\eta=0^+} = (1 - y_{F0})f_0,$$

$$\frac{1}{\Gamma}\left.\frac{d\theta_g}{d\eta}\right|_{\eta=0^+} = -lf_0 + \frac{J}{a^{1/2}}\left.\frac{d\theta_l}{dz}\right|_{z=-z_b} - \frac{N_l}{a^{1/2}}\int_{-z_b}^{0}(\theta_s-\theta_l)dz, \tag{7}$$

in which $l \equiv L/(c_pT_\infty) \gg 1$, since we consider a extreme low volatile fuel.
For the liquid phase of the problem, we have the following set of equations:

$$\varrho_l v_l = \frac{\bar{\dot{m}}}{\rho_\infty \bar{v}_\infty} \equiv \dot{m} \tag{8}$$

$$\varepsilon J\frac{d^2\theta_l}{dz^2} - \varepsilon M\frac{d\theta_l}{dz} = -N_l(\theta_s-\theta_l), \tag{9}$$

$$(1-\varepsilon)\frac{d^2\theta_s}{dz^2} = N_l(\theta_s-\theta_l) \tag{10}$$

The above parameters are given by:

$$M \equiv \dot{m}(c_l/c_p), \quad J \equiv (\bar{\lambda}_l/\bar{\lambda}_s),$$

The Clapeyron relation relates the fuel mass fraction at the liquid surface with the corresponding temperature as

$$y_{F0} = exp\left[l_R\left(\frac{1}{\theta_{l0}} - \frac{1}{\theta_b}\right)\right] \tag{11}$$

the parameter l_R is defined as $l_R \equiv L/(RT_\infty) \gg 1$.
The boundary conditions in the inlet liquid fuel are ($z \to -\infty$)

$$v_l - v_{l-\infty} = \theta_l - \theta_{-\infty} = \theta_s - \theta_{-\infty} = \varrho_l - (\rho_l/\rho_\infty) = y_F - 1 = 0$$

The velocity of the fuel in the gas phase at the liquid surface is related with the vaporization rate as

$$-a^{1/2}f_0 = \varrho_l\, v_{l0} = \dot{m} \tag{12}$$

The liquid temperature θ_{l0} at the interface liquid-gas is very close to that of boiling, but the solid phase temperature θ_{s0} is higher than that. The value for θ_{s0} will be obtained from the solid temperature profile coupling between the gas and liquid problem.

3. SOLUTIONS

The problem presents several scales, for the gas-solid region as for the liquid-solid region. Those two regions will be solved and their coupling will come from energy conservation condition at the interface. The assumption of low-porosity medium will appear as we consider $1/(\kappa\Gamma) = \beta\Gamma$, β being a unitary order parameter.

3.1 Gas-solid region

Above the interface, we must solve Eqs. (1) - (6) with proper boundary conditions. In this region, we recognize two distinct zones: one where viscous effects are not observed, denoted outer zone, and one at near the interface liquid-gas, where viscous effects becomes relevant. These two zones will be solved separately, but they must couple at proper limits.

In the outer zone, viscous effects are not significant. We perform a expansion for f given by $f = f_{(0)} + \Gamma^{-1}f_{(1)} + O(\Gamma^{-2})$, and obtain, from Eq. (2):

$$f'_{(0)} = 1 \tag{13}$$

$$f_{(0)}f''_{(0)} - \left(f'_{(0)}\right)^2 - \varepsilon Pr\beta f'_{(1)} = -\varepsilon Pr \tag{14}$$

The boundary conditions at the outer zone are given by:

$$f_{(0)}(0) = f_{(1)}(0) = 0,$$

$$\left.\frac{df_{(0)}}{d\eta}\right|_\infty = 1, \quad \left.\frac{df_{(1)}}{d\eta}\right|_\infty = U_1$$

U_1 is the higher order correction from the expansion of the boundary for U and will be from Eq. (14).

Solving the above set of equations, we obtain the momentum for the outer zone:

$$f(\eta) = \eta - \Gamma^{-1}\left(\frac{1-\varepsilon Pr}{1-\varepsilon}\right)\frac{\gamma}{\beta Pr}\,\eta + O\left(\Gamma^{-2}\right) \tag{15}$$

In this outer zone, gas and solid are in thermal equilibrium, since we assume that the interphase heat exchange is high. We quantify this by assuming $\theta_g \sim \theta_s$ and utilizing a single variable θ for both phases.

Performing a expansion in θ and utilizing the expression for f, we obtain from Eqs. (3) and (4), defining $\gamma = (1-\varepsilon)/\varepsilon$:

$$\gamma\theta_{(0)}^{''} + \eta\theta_{(0)}^{'} = 0, \tag{16}$$

$$\theta_{(0)}^{''} + \gamma\theta_{(1)}^{''} + \eta\theta_{(1)}^{'} - \eta\left(\frac{1-\varepsilon Pr}{1-\varepsilon}\right)\frac{\gamma}{\beta Pr}\theta_{(0)}^{'} = 0 \tag{17}$$

The boundary conditions are given by:

$$\theta_{(0)}(0) = \theta_m, \quad \theta_{(1)}(0) = \theta_{m1},$$

$$\theta_{(0)}(\eta \to \infty) = 1, \quad \theta_{(1)}(\eta \to \infty) = 0$$

In the large scale we are not able to enter the inner zone (at the interface the temperature is different for solid and gas, the inner zone will contemplate this decoupling). In order to couple solutions, we will develop the outer zone solution with the inner zone solution to obtain the temperature (θ_m and it's correction θ_{m1}) at an intermediary point.

The temperature at the outer zone is then given by:

$$\theta(\eta) = \theta_m + (1-\theta_m)\,erf\left(\frac{\eta}{\sqrt{2\gamma}}\right) - \Gamma^{-1}\left[\frac{(1-\theta_m)}{2\gamma}\sqrt{\frac{2}{\pi\gamma}}\left(1 + \frac{1-\varepsilon Pr}{1-\varepsilon}\frac{\gamma^2}{\beta Pr}\right)\eta\, exp\left(-\frac{\eta^2}{2\gamma}\right) - \right.$$

$$\left.\theta_{m1}\left(1 - erf\left(\frac{\eta}{\sqrt{2\gamma}}\right)\right)\right] + O\left(\Gamma^{-2}\right) \tag{18}$$

When we analyze the problem close to the interface, we are entering the inner zone. In this zone, viscous effects become important and we observe a decoupling between the temperature profiles.

We perform a coordinate change given by $\tilde{\eta} = \Gamma\eta$ and re-scale the momentum variable also as $\tilde{f} = \Gamma f$, since in the inner zone f is very small. Note that when we consider f as being small, we are in the regime of low order vaporization rate, hence, reinforcing the fact that the flame have extinguished, since if we have a small vaporization rate, the flame cannot sustain itself.

The interphase heat exchange is quantified by considering $N_v = \Gamma\, n_v$, where n_v is a unitary order parameter.

Performing the coordinate change, the re-scaling and expanding $\tilde{f} = \tilde{f}_{i(0)} + \Gamma^{-1}\tilde{f}_{i(1)} + O(\Gamma^{-2})$, after collecting equal powers, we obtain:

$$\tilde{f}_{i(0)}^{'''} - \varepsilon\beta\left(\tilde{f}_{i(0)}^{'} - 1\right) = 0 \tag{19}$$

$$Pr\tilde{f}_{i(1)}^{'''} + \tilde{f}_{i(0)}\tilde{f}_{i(0)}^{''} - \left(\tilde{f}_{i(0)}^{'}\right)^2 - \varepsilon\beta Pr\tilde{f}_{i(1)}^{'} = -\varepsilon Pr \tag{20}$$

The boundary conditions are:

$$\tilde{f}_{i(0)}(0) = \tilde{f}_0 = \Gamma f_0, \quad \left.\frac{d\tilde{f}_{i(0)}}{d\tilde{\eta}}\right|_0 = 0, \quad \left.\frac{d\tilde{f}_{i(0)}}{d\tilde{\eta}}\right|_\infty = \left.\frac{df_0}{d\eta}\right|_0 = 1,$$

$$\tilde{f}_{i(1)}(0) = 0, \quad \left.\frac{d\tilde{f}_{i(1)}}{d\tilde{\eta}}\right|_0 = 0, \quad \left.\frac{d\tilde{f}_{i(1)}}{d\tilde{\eta}}\right|_\infty = \left.\frac{df_1}{d\eta}\right|_0 = -\left(\frac{1-\varepsilon Pr}{1-\varepsilon}\right)\frac{\gamma}{\beta Pr}$$

Solving the above set of equations, we obtain the momentum in the inner zone:

$$\tilde{f}(\tilde{\eta}) = \tilde{\eta} + \frac{1}{\sqrt{\varepsilon\beta}}\left(exp\left(-\sqrt{\varepsilon\beta}\tilde{\eta}\right) - 1\right) + \tilde{f}_0 + \Gamma^{-1}\frac{1}{8\varepsilon\beta Pr}\left[8(\varepsilon Pr - 1)\tilde{\eta} - exp\left(-\sqrt{\varepsilon\beta}\tilde{\eta}\right)\left(10\tilde{\eta} + 2\sqrt{\varepsilon\beta}\tilde{\eta}^2\right) - \right.$$

$$\left.\left(exp\left(-\sqrt{\varepsilon\beta}\tilde{\eta}\right) - 1\right)\frac{10 + 8\,(1-\varepsilon Pr)}{\sqrt{\varepsilon\beta}}\right] + O\left(\Gamma^{-2}\right) \tag{21}$$

In the inner zone, the temperature profiles decouple and we observe a different behavior for each phase, solid and gas. At the interface, the solid temperature is higher than the gas temperature, a result that will be shown when we obtain the values for θ_{s0}, θ_m and θ_{m1}.

The equations to be solved are Eqs. (5) and (6). The coordinate $\tilde{\eta}$ is used also, and we perform expansion in both temperature variables, and after collecting equal powers, we obtain a set of four equations:

$$\varepsilon\theta''_{g(0)} = -\, n_v \left(\theta_{s(0)} - \theta_{g(0)}\right), \tag{22}$$

$$\varepsilon\theta''_{g(1)} + \varepsilon\tilde{f}_{i(0)}\theta'_{g(0)} = -\, n_v \left(\theta_{s(1)} - \theta_{g(1)}\right) \tag{23}$$

$$(1-\varepsilon)\theta''_{s(0)} = 0, \tag{24}$$

$$(1-\varepsilon)\theta''_{s(1)} = n_v \left(\theta_{s(0)} - \theta_{g(0)}\right) \tag{25}$$

With boundary conditions given by:

$$\theta_{g(0)}(0) = \theta_b, \quad \theta_{s(0)}(0) = \theta_{s0},$$

$$\theta_{g(1)}(0) = \theta_{s(1)}(0) = 0$$

The solutions also must obey a matching flux condition with the outer zone flux.
Solving the above set of equations, we obtain:

$$\theta_g(\tilde{\eta}) = \theta_{s0} + (1-\theta_m)\sqrt{\frac{2}{\pi\gamma}}\tilde{\eta} - (\theta_{s0}-\theta_b)\, exp\left(-\sqrt{\frac{n_v}{\varepsilon}}\tilde{\eta}\right) + \Gamma^{-1}\left[\frac{\varepsilon}{n_v}\left((1-\theta_m)\sqrt{\frac{2}{\pi\gamma}}\left(\tilde{f}_0 - \frac{1}{\sqrt{\varepsilon\beta}}\right) + \right.\right.$$

$$\left.\frac{\theta_{s0}-\theta_b}{1-\varepsilon}\right)\left(e^{-\sqrt{\frac{n_v}{\varepsilon}}\tilde{\eta}} - 1\right) - \left(\frac{1-\theta_m}{2\gamma}\sqrt{\frac{2}{\pi\gamma}}\left(1 + \frac{1-\varepsilon Pr}{1-\varepsilon}\frac{\gamma^2}{\beta Pr}\right) + \theta_{m1}\sqrt{\frac{2}{\pi\gamma}}\right)\tilde{\eta} - \frac{\theta_{s0}-\theta_b}{2\sqrt{\varepsilon\beta}}\left(\tilde{f}_0 - \right.$$

$$\left.\left.1 - \varepsilon\sqrt{\frac{\beta}{n_v}}\left(\frac{1}{1-\varepsilon} + \frac{\sqrt{\varepsilon}+\sqrt{n_v}\tilde{\eta}}{2\sqrt{\varepsilon}}\right)\right)\tilde{\eta}\, e^{-\sqrt{\frac{n_v}{\varepsilon}}\tilde{\eta}} + \frac{\sqrt{n_v}}{\varepsilon\beta}\frac{(\theta_{s0}-\theta_b)}{(2\sqrt{n_v}+\varepsilon\sqrt{\beta})}e^{-\sqrt{\frac{n_v}{\varepsilon}}\tilde{\eta}}\left(e^{-\sqrt{\varepsilon\beta}\tilde{\eta}} - 1\right)\right] + O\left(\Gamma^{-2}\right) \tag{26}$$

And for the solid phase:

$$\theta_s(\tilde{\eta}) = \theta_{s0} + (1-\theta_m)\sqrt{\frac{2}{\pi\gamma}}\tilde{\eta} - \Gamma^{-1}\left[\left(\frac{1-\theta_m}{2\gamma}\sqrt{\frac{2}{\pi\gamma}}\left(1 + \frac{1-\varepsilon Pr}{1-\varepsilon}\frac{\gamma^2}{\beta Pr}\right) + \theta_{m1}\sqrt{\frac{2}{\pi\gamma}}\right)\tilde{\eta} - \right.$$

$$\left.\frac{(\theta_{s0}-\theta_b)}{\gamma}\frac{1}{n_v}\left(e^{-\sqrt{\frac{n_v}{\varepsilon}}\tilde{\eta}} - 1\right)\right] + O\left(\Gamma^{-2}\right) \tag{27}$$

In the equation for the gas phase in the inner zone, we made use of the fact that the difference $(1-\theta_m)$ is very small, as will be seen forward, hence, we actually solved a simplified version of Eq. (23).

3.2 Liquid-solid region

For the liquid phase problem, we must analyze only Eqs. (9) and (10) with the proper boundary conditions. We re-scale N_l as $N_l = n_l\Gamma^2$, where n_l is a unitary order parameter, as we consider a high interphase heat exchange. With this in mind, we will decouple the liquid phase problem into two characteristic zones: a equilibrium and a boiling zone.

In the equilibrium zone, liquid fuel and solid matrix are in thermal equilibrium, and as in the case for the outer zone in the gas phase problem, we consider both temperatures as equal. With this in mind, we utilize Eqs. (9) and (10) to obtain:

$$\frac{(J+\gamma)}{M}\frac{d^2\theta}{dz^2} - \frac{d\theta}{dz} = 0 \tag{28}$$

Which must satisfy the conditions:

$$\theta(z \to -\infty) = \theta_{-\infty}, \quad \theta(z=0) = \theta_b$$

So, for the equilibrium region, the temperature profile is given by:

$$\theta(z) = (\theta_b - \theta_{-\infty})e^{z/r_1} + \theta_{-\infty} \tag{29}$$

where $r_1 = (J+\gamma)/M$.

When we reach the boiling zone, the profiles decouple, since the liquid reaches the boiling temperature and the heat provided to this phase is used to the phase change. The solid, however, continue to raise it's temperature, since it has no upper limit. So, when we reach the interface, the solid temperature is higher than the liquid temperature.

To analyze such zone, we perform a coordinate change given by $\tilde{z} = \Gamma z$ and a expansion given by:

$\theta_s = \theta_{s(0)} + \Gamma^{-1}\theta_{s(1)} + O(\Gamma^{-2})$,

$\theta_l = \theta_b - \Gamma^{-1}\theta_{l(1)} + O(\Gamma^{-2})$

With this, the governing equations are given by:

$$(1-\varepsilon)\frac{d^2\theta_{s(0)}}{d\tilde{z}^2} = n_l\left(\theta_{s(0)} - \theta_b\right) \tag{30}$$

$$(1-\varepsilon)\frac{d^2\theta_{s(1)}}{d\tilde{z}^2} = n_l(\theta_{s(1)} + \theta_{l(1)}) \tag{31}$$

And for the liquid phase, we only have a equation for the higher order correction, since the leading order is constant-valued:

$$-\varepsilon J\frac{d^2\theta_{l(1)}}{d\tilde{z}^2} = -n_l(\theta_{s(1)} + \theta_{l(1)}) \tag{32}$$

The boundary conditions are:

$\theta_{s(0)}(0) = \theta_{s0}, \quad \theta_{s(0)}(\tilde{z}\to-\infty) = \theta(z=0)$,

$\theta_{s(1)}(0) = \theta_{l(1)}(0) = 0, \quad \left.\frac{d\theta_{s(1)}}{d\tilde{z}}\right|_{-\infty} = -\left.\frac{d\theta_{l(1)}}{d\tilde{z}}\right|_{-\infty} = \left.\frac{d\theta}{dz}\right|_{0^-} = \frac{(\theta_b - \theta_{-\infty})}{r_1}$

The temperature profiles in the inner zone will be given then by:

$$\theta_s(\tilde{z}) = \theta_b + (\theta_{s0} - \theta_b)\ exp\left(\sqrt{\frac{n_l}{1-\varepsilon}}\tilde{z}\right) + \Gamma^{-1}\left(\frac{\theta_b - \theta_{-\infty}}{r_1}\right)\tilde{z} + O\left(\Gamma^{-2}\right) \tag{33}$$

$$\theta_l = \theta_b + \Gamma^{-1}\left(\frac{\theta_b - \theta_{-\infty}}{r_1}\right)\tilde{z} + O\left(\Gamma^{-2}\right) \tag{34}$$

The continuity for the heat flux in the leading order for the solid phase is not obeyed because when one enters the boiling zone the heat provided by the solid phase in this region is used for the liquid phase change.

From the condition of energy conservation at the interface and from the matching flux of thermal energy of solid phase from the gas problem with the liquid problem, we obtain the undetermined values θ_{s0}, θ_m and θ_{m1}.

Considering the continuity of the higher order heat flux of the solid phase at the interface, and the higher order correction in Eq. (37):

$$\theta_{s0} = \theta_b + \frac{\sqrt{\varepsilon(1-\varepsilon)}}{\sqrt{(1-\varepsilon)n_v} + \sqrt{\varepsilon\, n_l}}\frac{(\theta_b - \theta_{-\infty})}{J+\gamma}\frac{J}{a^{1/2}}M \tag{35}$$

$$\theta_m = 1 - \sqrt{\frac{\pi}{2}}\frac{\sqrt{n_l\gamma}}{\sqrt{n_v\gamma} + \sqrt{n_l}}\frac{(\theta_b - \theta_{-\infty})}{J+\gamma}\frac{J}{a^{1/2}}M \tag{36}$$

In the present problem we are considering a very low volatile fuel, so we re-write $l = \Gamma^2\tilde{l}$. With this, Eq. (7), re-scaled, is given by:

$$\left.\frac{d\theta_g}{d\tilde{\eta}}\right|_{\tilde{\eta}=0^+} = -\Gamma\,\tilde{l}\tilde{f}_0 + \Gamma\frac{J}{a^{1/2}}\left.\frac{d\theta_l}{d\tilde{z}}\right|_{\tilde{z}=-\infty} - \Gamma\left(\frac{n_l}{a}\right)^{1/2}(\theta_{s0} - \theta_b)\,(1-\varepsilon)^{1/2} \tag{37}$$

Where we already evaluated the integral term that corresponds to the heat exchange between solid and liquid at the boiling zone, this heat exchange is the responsible for the vaporization process.

From this, we estimate the vaporization rate as:

$$\tilde{f}_0 = -\left(\frac{n_l}{a}\right)^{1/2}\frac{(\theta_{s0} - \theta_b)}{\tilde{l}}\,(1-\varepsilon)^{1/2} \tag{38}$$

And from the coupling condition at higher order correction of the solid phase, we obtain:

$$\theta_{m1} = -\sqrt{\frac{\pi\gamma}{2}}\sqrt{\frac{n_v}{\varepsilon}}\frac{(\theta_{s0} - \theta_b)}{\gamma\, n_v} - \frac{(1-\theta_m)}{2\gamma}\left(1 + \left(\frac{1-\varepsilon Pr}{1-\varepsilon}\right)\frac{\gamma^2}{\beta Pr}\right) - \sqrt{\frac{\pi\gamma}{2}}\frac{(\theta_b - \theta_{-\infty})}{J+\gamma}\,M \tag{39}$$

With those values, the whole coupled problem have been solved, in all scales. In the next section, graphic results will be presented, so as their analysis.

4. RESULTS AND DISCUSSION

In the gas-solid region we observe two distinct zones: an outer zone and an inner zone. In the outer zone, viscous effects are not observed, since they occur near the liquid surface.

Analyzing the problem in this region, we observe a equal temperature profile for both gas and solid. This is due to the fact that at this scale, the heat exchange brings the temperature to a balance quickly. Also, one is not able to observe temperature variations occurring at the inner zone, and when we approach the inner zone, is observed an intermediary value $\theta_m + \Gamma^{-1}\theta_{m1} + O(\Gamma^{-2})$.

For the plotted figures below, we considered $\theta_b = 0.5$ and $\theta_{-\infty} = 0.25$. The parameters β, Pr, n_l, n_v, J and M are considered equal to 1 and the porosity used is 0.3. With those values, we obtain that $\theta_m \sim 0.943$, $\theta_{m1} \sim -0.259$, $\theta_{s0} \sim 0.525$ and $\tilde{f}_0 \sim -0.021$.

The outer zone behavior is observed in Figs. (2) and (3) for both momentum and temperature profiles.

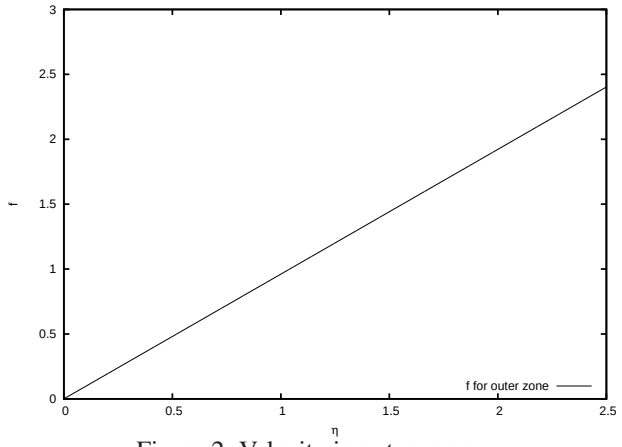

Figure 2. Velocity in outer zone

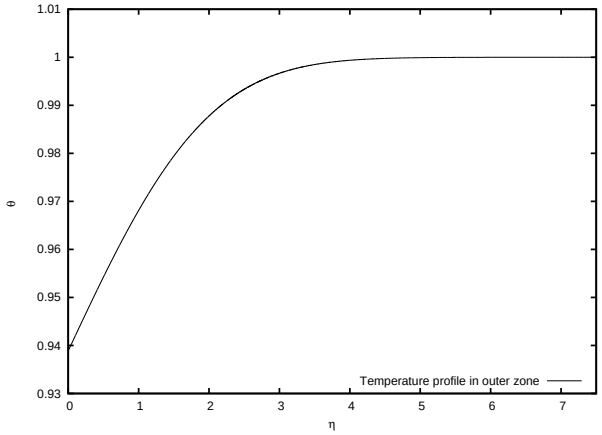

Figure 3. Temperature in outer zone

When we change the observable scale and enter the inner zone, viscous effects become relevant, as we can observe from Fig. (4). Also, it is possible to capture the decoupling between temperature profiles for gas and solid. Near the interface, heat transport for gas and solid are significantly different. This fact arise from their different-valued thermal conductivities, that is responsible for the observable decoupling, as we can see from Fig. (5).

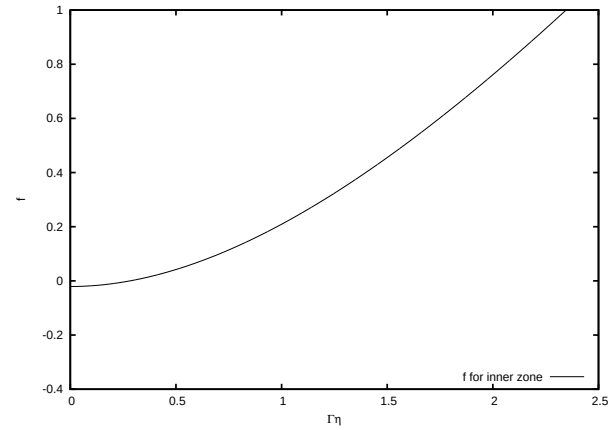

Figure 4. Velocity in inner zone

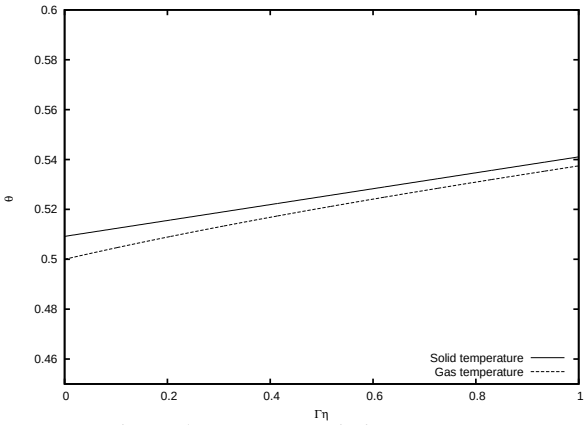

Figure 5. Temperature in inner zone

At the liquid-solid region we also observe two distinct zones: an equilibrium and a boiling zone. Far from the interface, we observe that the very high interphase heat exchange is responsible from bringing temperatures into equilibrium. Like in the outer zone case analyzed in the gas-solid problem, we observe a equal behavior for liquid and solid temperature in this equilibrium region. Both phases sense a exponential growth in their temperatures profiles, as one can see from Fig. (6).

When the profiles reach approximately the boiling fuel temperature, we observe their decoupling. At this temperature, all the heat provided to the liquid fuel will be used to the phase change process, while the solid porous matrix do not have such restrain. The observable effect is this profile decoupling, as the temperature for the solid phase continues to raise, until it reaches the interface temperature θ_{s0}, a higher value than $\theta_{l0} = \theta_b$, as we can see from Fig. (7). This difference

between solid and liquid temperature in the boiling zone is the responsible for the vaporization process, as we obtained from Eq. (37).

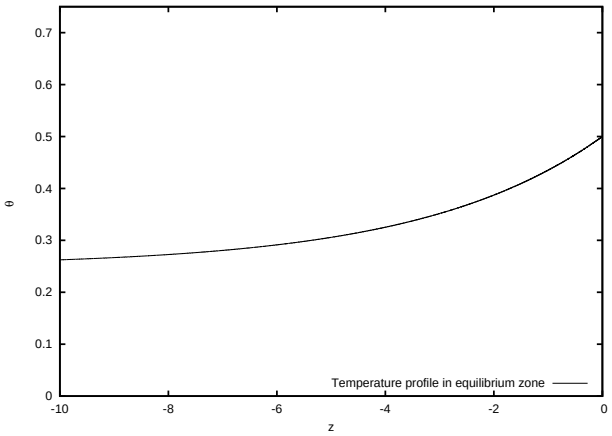

Figure 6. Temperature in equilibrium zone

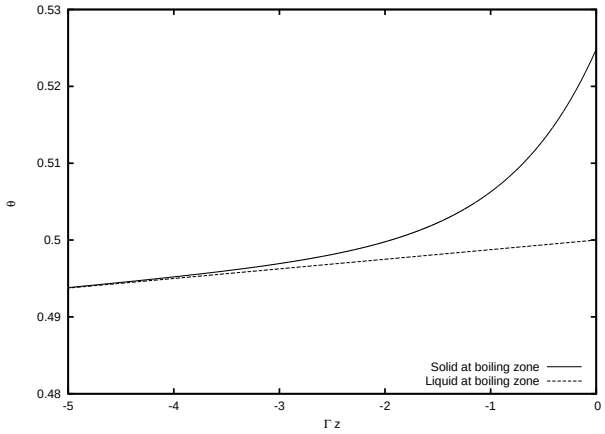

Figure 7. Temperatures in boiling zone

The vaporization rate, as given by Eq. (38), dependence over the medium porosity and the strain-rate is shown by Fig. (8).

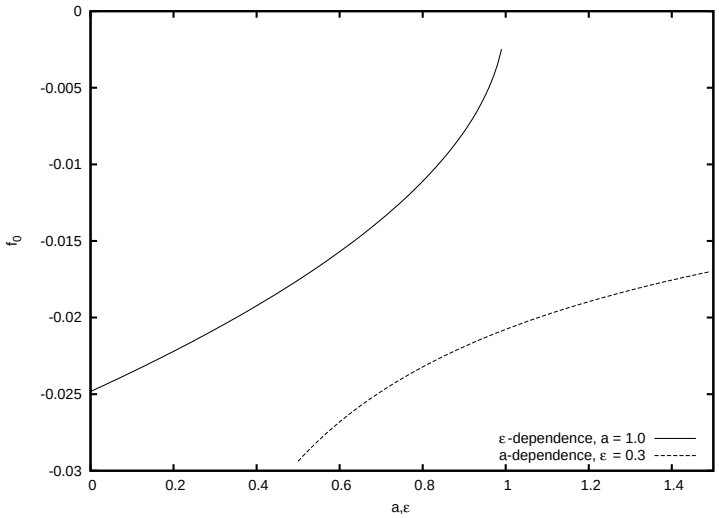

Figure 8. Vaporization rate

5. CONCLUSIONS

A flamelet formulation for the problem of the end of a diffusion flame of liquid fuel inside a low porosity porous medium was presented and analyzed analytically. In the final stage of the diffusion flame studied, the remaining fuel is a heavy, very low-volatile one and the relevant physical process is the vaporization. Since the vaporization rate obtained is very small, it is not possible to sustain the flame under such conditions.

In this evaporating regime, we must solve two regions: one that corresponds to the gas-solid and another corresponding to the liquid-solid region. In both regions we have two distinct zones. Outer zone and inner zone for the gas-solid region, and equilibrium zone and boiling zone for the liquid-solid region.

In the gas-solid region, the outer zone doesn't consider the viscous effects occurring near the liquid-gas interface. Gas and solid remain in equilibrium due to the high value of the interphase heat exchange. In this outer zone, it is not possible to enter the inner zone and analyze viscous effects, and a coordinate change is necessary. In the inner zone, near the interface, temperature profiles decouple and the viscous effects are observed.

The solid matrix carries the heat to the interior of the liquid-solid region. Far below the interface, liquid and solid are in thermal equilibrium, due to the high interphase heat exchange. As they approach the interface, we enter the boiling zone and solid and liquid profiles decouple, since the liquid reaches the boiling temperature and in this situation, all heat delivered to the liquid fuel will be used in phase change. The solid phase does not have such restrain, so it keeps raising

the temperature, until it reaches θ_{s0} at the interface. The interphase heat exchange in the boiling zone is the responsible for vaporizing the low volatility liquid fuel.

We performed an analytical analysis of the proposed, obtaining all relevant parameters and profiles for all regions and scales. Vaporization rate was estimated using energy conservation at the interface liquid-gas.

A very low volatile fuel have been assumed. If one assumes a highly volatile fuel, the vaporization process occur before the liquid reaches the boiling temperature, and the boiling zone collapses. To analyze such situation, one must consider a two-phase flow when the fuel starts to vaporize. Future works will consider highly volatility fuels, so as the combustion process itself.

6. ACKNOWLEDGEMENTS

This work was in part supported by Master in Science Program from Coordenação de Aperfeiçoamento de Pessoal de Nível Superior - CAPES.

7. REFERENCES

Castanier, L.M. and Brigham, W.E., 2003. "Upgrading of crude oil via in-situ combustion". *J. Petroleum Sci. & Eng.*, Vol. 39, pp. 125–136.

Howell, J.R., Hall, M.J. and Ellzey, J.L., 1996. "Combustion of hydrocarbons fuels within porous inert media". *Progr. Energy Combust. Sci.*, Vol. 22, pp. 121–145.

Kayal, T.K. and Chakravarty, M., 2005. "Combustion of liquid fuel inside inert porous media: an analytical approach". *Int. J. of Heat and Mass Transf.*, Vol. 48, pp. 331–339.

Mujeebu, M.A., Abdullah, M.Z., Bakar, M.Z.A., Mohamad, A.A., Muhad, R.M.N. and Abdullah, M.K., 2008. "Combustion in porous media and its applications - a comprehensive survey". *J. of Environ. Manag.*, Vol. 2, pp. 1–26.

Wu, Q., Weinbaum, S. and Andreopoulos, Y., 2005. "Stagnation-point flows in a porous medium". *Chemical Engineering Science*, Vol. 60, pp. 123–134.

8. Responsibility notice

The authors are the only responsible for the printed material included in this paper.